Hindawi
Advances in Civil Engineering
Volume 2021, Article ID 4002536, 9 pages
https://doi.org/10.1155/2021/4002536

Review Article

Mechanical Performance and Microstructure of Ultra-High-Performance Concrete Modified by Calcium Sulfoaluminate Cement

Meimei Song,[1,2] **Chuanlin Wang**,[3] **Ying Cui**,[1] **Qiu Li**,[2] **and Zhiyang Gao**[4]

[1]*School of Mechanical Engineering, Xi'an Shiyou University, Xi'an 710065, China*
[2]*State Key Laboratories of Silicate Materials for Architectures, Wuhan University of Technology, Wuhan 430070, China*
[3]*College of Engineering, Shantou University, Shantou, China*
[4]*Changjiang River Scientific Research Institute, Changjiang Water Resources Commission, Wuhan 430010, China*

Correspondence should be addressed to Qiu Li; qiu-li@whut.edu.cn

Received 6 July 2021; Revised 2 August 2021; Accepted 20 August 2021; Published 29 August 2021

Academic Editor: Tianyu Xie

High autogenous shrinkage property is one of the disadvantages of ultra-high-performance concrete (UHPC), which may induce early age cracking and threaten the safety of concrete structure. In the present study, different dosages of calcium sulfoaluminate (CSA) cement were added in UHPC as an effective expansive binder. Hydration mechanism, autogenous shrinkage property, and compressive strength of UHPC were carried out to investigate the effect of CSA addition on the mechanical properties of UHPC. Scanning electron microscopy was also employed to characterize the intrinsic microstructural reasons relating to the changes in macroproperties. Based on the XRD diagram, increasing formation of ettringite and $Ca(OH)_2$ can be found with increasing CSA content up to 15%. In the heat flow results of UHPC with 10% CSA addition, the maximum heat release increases to 2.6 mW/g, which is 8.3% higher than the reference UHPC, suggesting a higher degree of hydration with CSA addition. The results in autogenous shrinkage show that CSA expansion agent plays a significantly beneficial role in improving the autogenous shrinkage of UHPC. The corresponding autogenous shrinkage of UHPC is $-59.66\mu\varepsilon$, $-131.11\mu\varepsilon$, and $-182.31\mu\varepsilon$, respectively, at 7 d with 5%, 10%, and 15% addition, which is 108%, 117%, and 123% reduction compared to the reference specimen without CSA. In terms of compressive strength, UHPC with 5%, 10%, 15%, and 20% CSA addition has 10.5%, 17.4%, 30.2%, and 22.1% higher compressive strength than that for the reference UHPC at 28 d. Microstructural study shows that there is an extremely dense microstructure in both the bulk matrix and interfacial transition zone of UHPC with 10% CSA addition, which can be attributed to the higher autogenous shrinkage property and can therefore result in higher mechanical performance.

1. Introduction

With the development of super-high-rise and super-long-span building, durability and compressive strength of concrete are faced with great challenge [1, 2]. Under this circumstance, ultra-high performance concrete (UHPC) has aroused enormous attention due to its extremely high compressive strength of 80–150 MPa and superior durability [3, 4]. It is designed based on the theory of densified particle packing and internal defects (pores and microcracks) which are limited by improving the fineness and activity of the components [5]. In detail, the gap of millimeter size (e.g., aggregate) is filled by micron size particles (e.g., cement, fly ash, and mineral powder), and the gap of micron size is then filled by submicron size particles (e.g., silica fume and fly ash). However, due to a high proportion of cementitious materials (cement, 800–1000 kg/m^3) and low water-to-binder ratio of 0.15–0.3, hydration degree of UHPC is rather low [6]. More importantly, one of the most serious disadvantages of UHPC is high autogenous shrinkage property, which may cause early age cracking and therefore threaten the safety and service life of concrete structure [7–10].

In order to reduce the autogenous shrinkage of UHPC, additions of expansion agent, shrinkage reducing agent

(SRA), and super absorbent polymer (SAP) are often incorporated to replace part of cementitious materials at various proportions [11–13]. Among them, expansion agent is one of the most effective additives [13]. Lots of researches have been carried out to study the effect of different expansive additives on reducing the autogenous shrinkage of concrete [14, 15]. Among them, calcium sulfoaluminate (CSA) cement has generated a lot of interest [9, 10].

CSA cement was first produced in China in the 1970s by heating mixtures of limestone, bauxite, and gypsum at about 1250$\mu\varepsilon$, generating cement clinker with main compositions of calcium sulfoaluminate and belite. It was characterized as an effective expansive binder owning to the massive formation of crystalline ettringite during hydration [16, 17]. Furthermore, it also plays a beneficial role in improving the strength of UHPC [18]. Research by Yoo et al. [9] found out that CSA expansive agent played a positive role in reducing the expansive strains of UHPC and this increment grew with increasing CSA content. In detail, the shrinkage strains were 7% and 10% smaller with 6% and 8% CSA addition than plain UHPC after 15 d. Research by Shen et al. [19] showed that, with 15% CSA-CaO addition, the autogenous shrinkage of UHPC reduced 59% at 7 d compared to the plain UHPC. It was indicated that addition of CSA-CaO also plays a beneficial influence on the strength development. With 5% CSA-CaO addition, compressive strength of UHPC increased to 97 MPa, compared to 95 MPa in the reference specimen at 3 d; corresponding flexural strength improved from 27 MPa to 30 MPa.

To sum up, CSA cement is a kind of highly promising expansion agent and strength enhancer in the application of UHPC. But up to now, there is a lack of study on the effect of optimized CSA cement on the autogenous shrinkage, mechanical performance, and hydration mechanism of UHPC as well as the underlying microstructural changes, which is of great importance before wider application of UHPC modified by CSA cement can be made. In this study, different dosages of CSA cement (0%, 5%, 10%, 15%, and 20%) were added in UHPC to replace part of OPC cement, aiming at producing UHPC with higher strength and durability.

2. Materials and Experiment

2.1. Materials. Materials of ordinary Portland cement, CSA expansion agent, minerals of silica fume, fly ash, and slag were used to produce UHPC. Chemical compositions of each material are shown in Table 1. In this study, various proportions of CSA were added in UHPC to investigate its effect on the mechanical performance of UHPC. In detail, CSA addition of 0%, 5%, 10%, 15%, and 20% was prepared, designating CSA0, CSA5, CSA10, CSA15, and CSA20, respectively. The detailed mixing design is listed in Table 2. UHPC was cast in 100 mm × 100 mm × 515 mm for autogenous shrinkage testing, 100 mm × 100 mm × 100 mm for compressive strength testing, and 225 mm × 55 mm × 10 mm for bending performance testing. After 24 h, the specimens were demolded and cured under 20 ± 1°C with relative humidity of 95% until the investigated age.

2.2. Experimental Work

2.2.1. XRD and Heat Flow Analysis. In order to investigate the effect of CSA on the hydration of UHPC, corresponding pure UHPC pastes with different CSA contents (0%, 5%, 10%, 15%, and 20%) were prepared in cylinder molds. After 24 h, the specimens were cured in a water bath with the temperature set at 20 ± 1°C. At a curing age of 7 d, samples were fractured and then ground into fine powder in an agate mortar. XRD was undertaken by Bruker D8 using CuKα1 radiation with a working condition of 40 kV and 30 mA. Data of powder samples was collected in a 2θ range between 0° and 50° with a step size of 0.02°.

Cement hydration is an exothermic reaction, and the heat generated during the hydration may improve the autogenous shrinkage of UHPC. Therefore, investigation on the effect of CSA cement on the heat flow of UHPC is of great importance in controlling the autogenous shrinkage. In this study, multichannel isothermal calorimeter (model TAM Air, TA Instruments) was applied to investigate the heat flow in UHPC. During the tests, the isothermal temperature is 20 ± 0.02°C, and heat flow of UHPC was recorded at an early age up to 72 h.

2.2.2. Autogenous Shrinkage Test. In this study, autogenous shrinkage of UHPC was conducted according to the Chinese standard GB/T 50082-2009 [20]. During the tests, a noncontact deformation tester of concrete (model CABR-NES) was used (as shown in Figure 1), and UHPC specimens were covered with polyethylene film. At a curing age of 1 d, 2 d, 3 d, 5 d, 7 d, 14 d, 21 d, and 28 d, autogenous shrinkage of UHPC was tested.

2.2.3. Mechanical Strength Test. Mechanical properties of compressive strength and bending performance were examined in this study. Compressive strength of UHPC cured at 3 d, 7 d, and 28 d was examined according to the Chinese standard GB/T 50082-2009 [20], and three specimens were performed to get an average result. It was carried out by a universal strength testing machine at a loading rate of 2.4 kN/s, and the maximum load of the machine is 300 kN.

Bending performance of UHPC samples was tested by a four-point bending test using Tinius Olsen H25KS according to BS-EN 1170-5:1997 [21], with a major span of 200 mm and a load rate at 1.8 mm/min [22]. The detailed information on the experimental setup is shown in Figure 2. As a result, load-deflection curve of UHPC was obtained, and stress-strain curve can be subsequently acquired by calculation.

2.2.4. Microstructural Observation. In order to examine the intrinsic microstructural reasons underlying mechanical performance, microstructure of fractured UHPC cured at 20°C for 28 d was characterized by the secondary electron imaging mode in SEM. Before testing, hydration of UHPC specimens was stopped by soaking them in liquid nitrogen for few minutes and then placed in a freeze drier until constant weight can be maintained. In this study, JEOL JSM-

Table 1: Oxide compositions of the CSA and OPC cement powder (by wt. %).

	CaO	SiO_2	Al_2O_3	SO_3	Fe_2O_3	MgO	K_2O	Na_2O	TiO_2	SrO	BaO	Mn_3O_4	LOI*
CSA	42.33	9.00	33.82	8.83	1.35	2.29	0.22	0.12	1.61	0.07	0.02	0.03	0.31
OPC	62.14	19.42	4.83	4.81	1.95	2.13	0.75	0.24	0.24	0.07	0.02	0.07	3.33
SF	0.11	97.90	0.52	—	0.17	0.10	—	0.99	—	—	—	—	0.21
FA	3.83	60.84	23.73	0.63	6.96	0.55	—	—	—	—	—	—	3.46
GGBS	37.11	32.91	15.36	—	0.74	8.52	—	—	1.95	—	—	—	3.41

Note: SF: silica fume; FA: fly ash; GGBS: ground granulated blast furnace slag; LOI: loss on ignition.

Table 2: Mixing design of UHPC.

	OPC (kg/m^3)	CSA (kg/m^3)	SF (kg/m^3)	GGBS (kg/m^3)	FA (kg/m^3)	*w/b*	Sand (kg/m^3)	SP (%)	AA (%)
CSA0	857.4	0	53.6	53.6	107.1	0.24	1071.7	0.675	0.25
CSA5	816.6	40.8	53.6	53.6	107.1	0.24	1071.7	0.675	0.25
CSA10	779.4	77.9	53.6	53.6	107.1	0.24	1071.7	0.675	0.25
CSA15	745.6	111.8	53.6	53.6	107.1	0.24	1071.7	0.675	0.25
CSA20	714.5	142.9	53.6	53.6	107.1	0.24	1071.7	0.675	0.25

Note: *w/b*: water-to-binder ratio; SP: superplasticizer; AA: antifoaming agent.

5800LV equipped with energy dispersive X-ray microanalysis (EDX) was applied for microstructural observation, operating at an accelerating voltage of 20 kV and a working distance of 12 mm. EDX was also undertaken to investigate the relevant elemental information at specific spot.

3. Results and Discussion

3.1. XRD Analysis of UHPC Paste. XRD diffraction diagram of UHPC paste with 0%, 5%, 10%, 15%, and 20% CSA additions cured at 20 ± 1°C for 7 d is presented in Figure 3. Remnants of C_3S and C_2S can be observed, suggesting a lower hydration degree at this stage. This is because water to binder ratio is considerably low in UHPC in this study, which is only 0.24. On the other hand, hydration of calcium sulfoaluminate initiates rapidly at early age, consuming large proportion of water; therefore, there is insufficient free water available for the hydration of C_3S and C_2S. From the XRD diagram, it can also be seen that calcium sulfoaluminate is not traceable in each specimen. This is because hydration of calcium sulfoaluminate happens drastically in the first 1-2 h to 2 d, generating large amounts of ettringite formation as shown in equation (1). It can also be found that the main hydration products of UHPC are ettringite and $Ca(OH)_2$, both with and without CSA addition. In particular, the intensities of ettringite and $Ca(OH)_2$ peak increase with increasing CSA content up to 15%; however, the increment is prone to slow down with a larger CSA content of 20%. This is because, with a larger CSA content of 20%, larger proportions of water are consumed in the rapid hydration of calcium sulfoaluminate at early age, which leads to less free water available for the hydration of C_3S and C_2S $Ca(OH)_2$, so the reduced CH generation can be found in CSA20. However, according to the XRD diagram, reduced ettringite is also formed in CSA20. This phenomenon can be explained that, with the depletion of gypsum, monosulfate will be formed during the hydration of calcium sulfoaluminate as shown in equation (2), which requires less water molecule compared with that in equation (1). At the same time, in the absence of gypsum, part of ettringite will gradually transform into amorphous monosulfate, as shown in equation (3).

$$C_4A_3\overline{S} + 2CH\overline{S}_2 + 34H \longrightarrow C_3A \cdot 3C\overline{S} \cdot 32H + 4AH_3 \quad \text{(ettringite formation)} \tag{1}$$

$$C_4A_3\overline{S} + 18H \longrightarrow C_3A \cdot C\overline{S} \cdot 12H + 4AH_3 \quad \text{(monosulfate formation)} \tag{2}$$

$$C_3A \cdot 3C\overline{S} \cdot 32H + 2\left(C_3A \cdot 6H\right) \longrightarrow 3\left(C_3A \cdot C\overline{S} \cdot 12H\right) \quad \text{(monosulfate formation)} \tag{3}$$

3.2. Heat Flow of UHPC. The heat flow of UHPC with 10% CSA addition up to 72 h is illustrated in Figure 4. It is clear that, in the reference UHPC without CSA addition, there is a dormant period in the first 8 h; subsequently, an acceleration period follows denoted by a significantly strong peak between 8 h and 44 h. However, the heat flow of UHPC is considerably influenced by 10% CSA addition. In general, the heat flow of dormant period of cement hydration increases to 0.4 mW/g compared to a value of 0.32 mW/g in the reference. The main peak of the heat flow also advances to 13 h compared to 18 h for the reference UHPC. At the same time, the maximum heat flow value increases to

Figure 1: Testing equipment of autogenous shrinkage of UHPC.

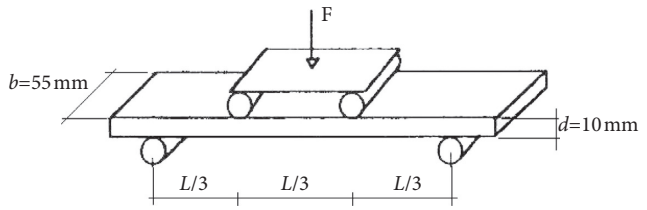

Figure 2: Experimental setup for bending performance tests of UHPC [21].

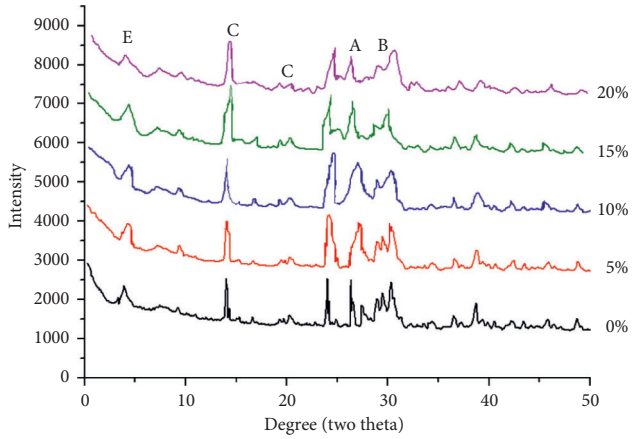

Figure 3: XRD diffraction diagram of UHPC with different CSA additions at 7 d (E: ettringite; C: $Ca(OH)_2$; A: C_3S; B: C_2S).

2.6 mW/g; this is 8.3% higher than the reference UHPC. This phenomenon indicates that there is an accelerated effect of CSA addition on the hydration process of UHPC at early age, and a higher degree of hydration can be achieved with CSA addition. This is because hydration of calcium sulfoaluminate initiates more rapidly and intensively than OPC in the first 48 h, which is an exothermic reaction and releases large proportions of hydration heat flow.

3.3. Autogenous Shrinkage of UHPC. The effect of CSA expansion agent on the autogenous shrinkage development of UHPC is presented in Figure 5. It can be seen that the reference UHPC with no CSA addition exhibits a considerably high shrinkage property, and the autogenous shrinkage reaches about 600$\mu\varepsilon$ at 1 d. This value is significantly reduced compared to 1500$\mu\varepsilon$ from a previous study by Shen et al. [19]. This is because a larger w/c ratio of 0.24 is used in this study compared to 0.18 in [19]. After 1 d, the increment demonstrates a tendency to slow down, reaching 638$\mu\varepsilon$ and 652$\mu\varepsilon$, respectively, at 2 d and 7 d. After 7 d, there is gradual increase in the shrinkage of reference UHPC, and it reaches about 800$\mu\varepsilon$ at 28 d. In conclusion, the autogenous shrinkage of plain UHPC in the present study increases rapidly at early age and then demonstrates a gradual growth later. This trend line of heat flow is in agreement with previous studies by Xie et al. [23] and Sobuz et al. [24].

From the results in Figure 5, it can be observed that the addition of CSA expansion agent plays a significantly beneficial role in improving the autogenous shrinkage of UHPC. All the specimens exhibit favorable expansion property in varying degrees, and the swelling property of UHPC tends to improve with an increasing CSA proportion between 5% and 15%. Specifically, the autogenous shrinkage of UHPC with 5%, 10%, and 15% addition of CSA is −59.66$\mu\varepsilon$, −131.11$\mu\varepsilon$, and −182.31$\mu\varepsilon$, respectively, at 7 d, which is 108%, 117%, and 123% reduction in autogenous shrinkage compared to the reference specimen. The data is comparable to the previous studies. For example, research by Xie et al. [23] showed that, with 2% SRA addition, 65.6% reduction in autogenous shrinkage can be achieved compared to the reference plain UHPC at 7 d. Similarly, Su et al. [25] reported an up to 95% reduction in autogenous shrinkage with 2% SRA dosage at 7 d.

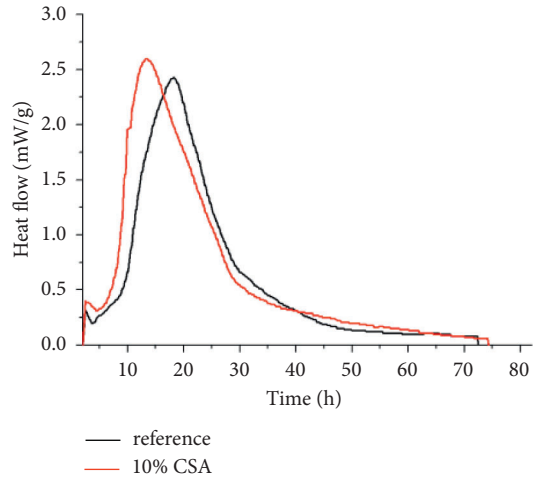

Figure 4: Effect of CSA addition on the heat flow of UHPC up to 72 h.

However, when the CSA proportion increases to 20%, superior expansive effect can still be found out but there is a slight reduction in the swelling property of UHPC. The corresponding autogenous shrinkage reduced to $-151.26\mu\varepsilon$ at 28 d, which is 9.24% lower than that with 15% CSA addition. This is because formation of CH and ettringite is the main reason relating to the expansive property of CSA cement; however, less amounts of CH and ettringite generation are observed according to the XRD diagram in Figure 3. Therefore, expansive property of UHPC is limited to some extent with 20% CSA addition. The result is in consistence with the previous studies [16, 19].

It can be concluded that CSA cement possesses great potential to reduce the autogenous shrinkage of UHPC, and a superior expansion property can be obtained with an optimized volume of 15%. This beneficial expansion property can be attributed to the continuous formation of expansive ettringite during hydration, and the swelling stress generated from ettringite may compensate the autogenous shrinkage developed in UHPC. The corresponding microstructural reasons are discussed in Section 3.4.

3.4. Mechanical Performance of UHPC. Compressive strengths of UHPC with different CSA additions are illustrated in Figure 6. It can be found out that addition of CSA is conducive to the improvement of compressive strength. In general, the rapidity of compressive strength increment is enhanced with CSA additions of 5–15%. However, the increasing speed tends to slow down at a higher CSA content of 20%, and there is a slight reduction compared to that with 15% CSA addition. This is because reduced amount of ettringite and $Ca(OH)_2$ is formed at this stage, both of which contribute significantly to the strength development of UHPC, as illustrated in the XRD analysis in Section 3.1. In detail, at the age of 3 d, compressive strength of UHPC is 74 MPa, 78 MPa, 87 MPa, and 84 MPa, respectively, with 5%, 10%, 15%, and 20% CSA addition, which is 4.2%, 9.8%, 22.5%, and 18.3% higher than that for the reference UHPC without CSA addition. With increasing ages, the compressive strength of different UHPC increases gradually. At 28 d, the corresponding compressive strength reaches 95 MPa, 101 MPa, 112 MPa, and 105 MPa with 5%, 10%, 15%, and 20% CSA addition, which is 10.5%, 17.4%, 30.2%, and 22.1% higher than that for the reference UHPC.

3.5. Microstructure of UHPC. Microstructure of UHPC with 10% CSA addition is shown in Figure 7. It can be observed that an extremely dense microstructure is developed in the bulk matrix, and large air voids are almost absent. This can be correlated to the expansive stress of ettringite generated during the hydration process, which may compensate the autogenous shrinkage of UHPC and lead to a compact and dense matrix to a great extent. This is consistent with the analysis of autogenous shrinkage in Section 3.3. Spherical structure of silica fume with a diameter of about 10μm can be observed, which suggests that silica fume mainly plays a physical filler effect in a microstructural view. In Figure 7(a), prismatic-shaped ettringite can be observed in the matrix, which is one of the main hydration products in the UHPC system used in this study. The corresponding EDX analysis on Spot "1" as shown in Figure 7(b) reveals a dominance of CaO (16.05 wt. %) and SiO_2 (9.81 wt. %) with small inclusions of SO_3 (5.83 wt. %) and Al_2O_3 (4.82 wt. %). The corresponding Al/Ca ratio is 0.33 and S/Ca ratio is 0.255, which might be the intermixtures of ettringite (Al/Ca = 0.33, S/Ca = 0.5) and small quantities of C-S-H gel.

At the same time, there is a dense and intimate contact between aggregate and cement at the interfacial transition zone in Figure 7(c). This can be attributed to the high autogenous shrinkage property CSA addition, which may significantly narrow the gaps between aggregate and cement. High-quality interfacial transition zone with less gaps and porosity is beneficial to higher mechanical performance of the UHPC, which is in consistence with the results in Section 3.3. This is in agreement with the previous research [26, 27], indicating that quality of interface is one of the key factors deciding the strength of concrete structure.

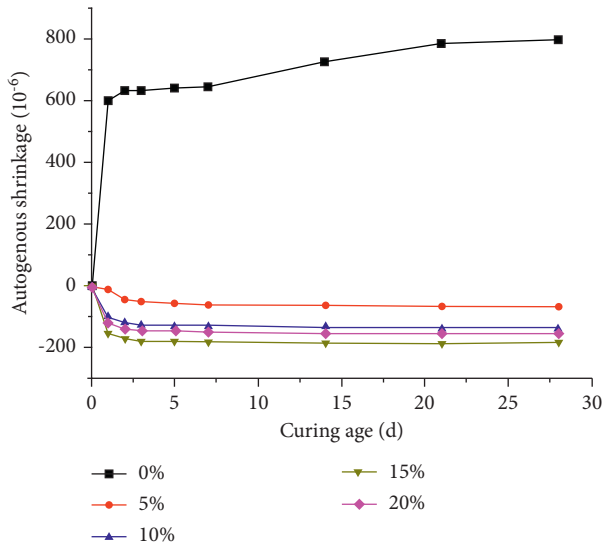

Figure 5: Autogenous shrinkage development of UHPC with different CSA additions.

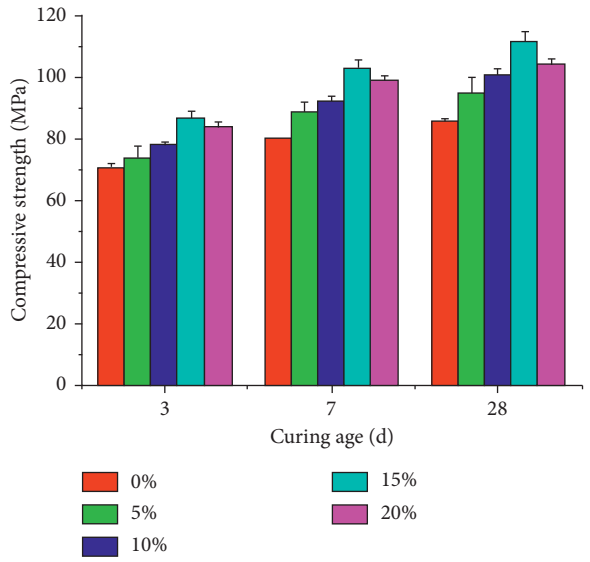

Figure 6: Compressive strength development of UHPC with different CSA additions.

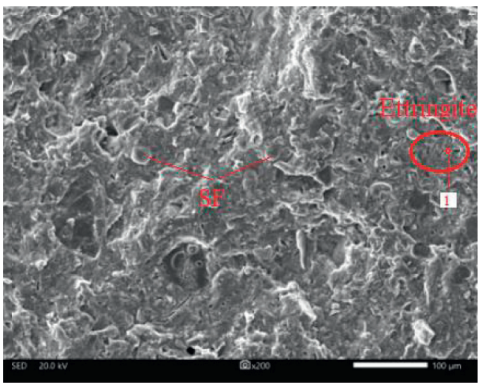

(a)

Figure 7: Continued.

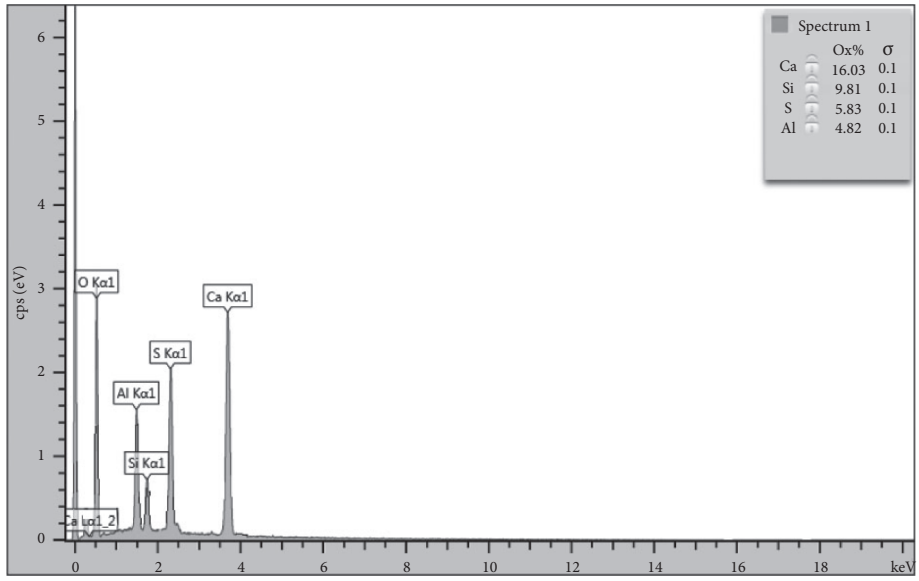

(b)

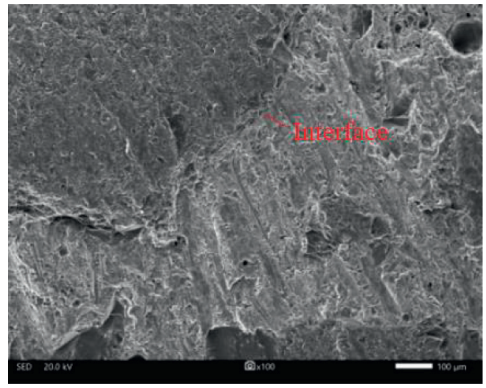

(c)

Figure 7: Microstructural features of UHPC with 10% CSA additions at 7 d. (a) Microstructure of bulk matrix. (b) Spot analysis on Spot "1". (c) Microstructure at the aggregate-cement interface.

4. Conclusion

XRD diagram indicates that the main hydration products of UHPC are ettringite and $Ca(OH)_2$, both with and without CSA addition. In particular, increasing formation of ettringite and $Ca(OH)_2$ can be found with increasing CSA content up to 15%. In the heat flow results of UHPC with 10% CSA addition, the maximum heat release increases to 2.6 mW/g, which is 8.3% higher than the reference UHPC. This is suggestive of an accelerated effect of CSA addition on the hydration process of UHPC at early age, and a higher degree of hydration can be achieved with CSA addition.

From the autogenous shrinkage results, it can be concluded that CSA expansion agent plays a significantly beneficial role in improving the autogenous shrinkage of UHPC, especially with an optimized addition between 5% and 15%. The autogenous shrinkage of UHPC with 5%, 10%, and 15% addition of CSA is $-59.66\mu\varepsilon$, $-131.11\mu\varepsilon$, and $-182.31\mu\varepsilon$, respectively, at 7 d, which is 108%, 117%, and 123% reduction compared to the reference specimen at the same age.

At the same time, addition of CSA expansion agent tends to increase the compressive strength of UHPC to a great extent. For example, compressive strength of UHPC with 5%, 10%, 15%, and 20% CSA addition is 4.2%, 9.8%, 22.5%, and 18.3%, respectively, higher than that for the reference UHPC without CSA addition. At 28 d, the corresponding increment rises to 10.5%, 17.4%, 30.2%, and 22.1%, respectively, compared to that for the reference sample.

Microstructural study shows that there is an extremely dense microstructure in UHPC with the addition of CSA, and large air voids are almost absent in the matrix. Spherical structure of silica fume is displayed in the bulk matrix, which suggests that it mainly plays a physical filler effect in a microstructural view. Prismatic-shaped ettringite can be observed in the matrix, intermixed with small quantities of C-S-H gel. At the same time, there is a dense and intimate contact between aggregate and cement at the interfacial transition zone, which can be attributed to the high autogenous shrinkage property CSA addition. High-quality interfacial transition zone with less gaps and porosity is

beneficial to higher mechanical performance of the UHPC; this is in agreement with the compressive strength results in this study.

Therefore, not only is CSA cement an effective expansive agent in the application of UHPC as long as the amount of admixture is controlled within reasonable range, but it also has beneficial effect on the strength development of UHPC.

Data Availability

The data used to support the findings of this study are available from the corresponding author upon request.

Conflicts of Interest

The authors declare that they have no conflicts of interest.

Acknowledgments

This work was supported by the State Key Laboratories of Silicate Materials for Architectures, Wuhan University of Technology in China (no. SYSJJ2019-17), Key Laboratory of Structure and Wind Tunnel of Guangdong Higher Education Institutes Open Fund (no. 202002), and the Natural Science Basic Research Program of Shaanxi Province (nos. 2021JQ-605 and 2020JM-536).

References

[1] R. Yu, P. Spiesz, and H. J. H. Brouwers, "Effect of nano-silica on the hydration and microstructure development of ultra-high performance concrete (UHPC) with a low binder amount," *Construction and Building Materials*, vol. 65, no. 9, pp. 140–150, 2014.

[2] M. Alkaysi and S. El-Tawil, "Effects of variations in the mix constituents of ultra high performance concrete (UHPC) on cost and performance," *Materials and Structures*, vol. 49, no. 10, pp. 4185–4200, 2016.

[3] S. Li and S. Cheng, L. Mo and M Deng, Effects of steel slag powder and expansive agent on the properties of ultra-high performance concrete (UHPC): based on a case study," *Materials*, vol. 13, no. 3, pp. 1–11, 2020.

[4] A. Tafraoui, G. Escadeillas, and T. Vidal, "Durability of the ultra high performances concrete containing metakaolin," *Construction and Building Materials*, vol. 112, pp. 980–987, 2016.

[5] D. Wang, C. Shi, Z. Wu, J. Xiao, Z. Huang, and Z. Fang, "A review on ultra high performance concrete: Part II. Hydration, microstructure and properties," *Construction and Building Materials*, vol. 96, pp. 368–377, 2015.

[6] J. Li, Z. Wu, C. Shi, and Q. Yuan, "Durability of ultra-high performance concrete-a review," *Construction and Building Materials*, vol. 255, Article ID 119296, 2020.

[7] J. J. Park, S. W. Kim, G. S. Ryu, and K. M. Lee, "The influence of chemical admixtures on the autogenous shrinkage ultra-high performance concrete," *Key Engineering Materials*, vol. 452-453, pp. 725–728, 2011.

[8] A. M. Soliman and M. L. Nehdi, "Effect of drying conditions on autogenous shrinkage in ultra-high performance concrete at early-age," *Materials and Structures*, vol. 44, no. 5, pp. 879–899, 2011.

[9] D.-Y. Yoo, S. Kim, J.-Y. Lee, I. You, and S.-J. Lee, "Implication of calcium sulfoaluminate-based expansive agent on tensile behavior of ultra-high-performance fiber-reinforced concrete," *Construction and Building Materials*, vol. 217, pp. 679–693, 2019.

[10] D.-Y. Yoo, B. Chun, and J.-J. Kim, "Effect of calcium sulfoaluminate-based expansive agent on rate dependent pullout behavior of straight steel fiber embedded in UHPC," *Cement and Concrete Research*, vol. 122, pp. 196–211, 2019.

[11] A. M. Soliman and M. L. Nehdi, "Effect of partially hydrated cementitious materials on early-age shrinkage of ultra-high-performance concrete," *Magazine of Concrete Research*, vol. 65, no. 19-20, pp. 1147–1154, 2013.

[12] J. Liu, Z. Ou, J. Mo, Y. Chen, T. Guo, and W. Deng, "Effectiveness of saturated coral aggregate and shrinkage reducing admixture on the autogenous shrinkage of ultrahigh performance concrete," *Advances in Materials Science and Engineering*, vol. 2017, Article ID 2703264, 11 pages, 2017.

[13] V. Mechtcherine, M. Gorges, C. Schroefl et al., "Effect of internal curing by using superabsorbent polymers (SAP) on autogenous shrinkage and other properties of a high-performance fine-grained concrete: results of a RILEM round-robin test," *Materials and Structures*, vol. 47, no. 3, pp. 541–562, 2014.

[14] J. J. Feng, C. L. Zhou, Y. Sun, and X. Q. Wang, "The influence of curing temperature on the coordination of the expansion and strength of high strength expansive concrete," *Key Engineering Materials*, vol. 539, pp. 205–210, 2013.

[15] J.-K. Kim and C.-S. Lee, "Prediction of differential drying shrinkage in concrete," *Cement and Concrete Research*, vol. 28, no. 7, pp. 985–994, 1998.

[16] P. Chaunsali, P. Mondal, and J. Bullard, "Influence of calcium sulfoaluminate (CSA) cement content on expansion and hydration behavior of various ordinary Portland cement-CSA blends," *Journal of the American Ceramic Society*, vol. 98, no. 8, pp. 2617–2624, 2015.

[17] P. K. Mehta, "Expansion characteristics of calcium sulfoaluminate hydrates," *Journal of the American Ceramic Society*, vol. 50, no. 4, pp. 204–208, 2010.

[18] F. P. Glasser and L. Zhang, "High-performance cement matrices based on calcium sulfoaluminate-belite compositions," *Cement and Concrete Research*, vol. 31, no. 12, pp. 1881–1886, 2001.

[19] P. Shen, L. Lu, Y. He et al., "Investigation on expansion effect of the expansive agents in ultra-high performance concrete," *Cement and Concrete Composites*, vol. 105, p. 103425, 2020.

[20] GB/T 50082-2009, *Standards for Test Methods of Long-Term Performance and Durability of Ordinary Concrete*, National Standards of the People's Republic of China, China Construction Industry Press, Beijing, China, 2009.

[21] BS-EN 1170-5:1997, *Precast Concrete Products-Test Methods for Glass-Fibre Reinforced Cement*, British Standard, British Standard Institute, Bengaluru, Karnataka, 1997.

[22] M. Song, P. Purnell, and I. Richardson, "Microstructure of interface between fibre and matrix in 10-year aged GRC modified by calcium sulfoaluminate cement," *Cement and Concrete Research*, vol. 76, pp. 20–26, 2015.

[23] T. Xie, C. Fang, M. S. Mohamad Ali, and P. Visintin, "Characterizations of autogenous and drying shrinkage of ultra-high performance concrete (UHPC): an experimental study," *Cement and Concrete Composites*, vol. 91, pp. 156–173, 2018.

[24] H. R. Sobuz, P. Visintin, M. S. Mohamed Ali, M. Singh, M. C. Griffith, and A. H. Sheikh, "Manufacturing ultra-high performance concrete utilising conventional materials and

production methods," *Construction and Building Materials*, vol. 111, pp. 251–261, 2016.

[25] S. Treesuwan, K. Maleesee, and S. Zhang, "Effects of shrinkage reducing agent and expansive additive on mortar properties," *Advances in Materials Science and Engineering*, vol. 2017, Article ID 8917957, 11 pages, 2017.

[26] D. Neff, J. Harnisch, M. Beck, V. L'Hostis, J. Goebbels, and D. Meinel, "Morphology of corrosion products of steel in concrete under macro-cell and self-corrosion conditions," *Materials and Corrosion*, vol. 62, no. 9, pp. 861–871, 2015.

[27] A. T. Horne, I. G. Richardson, and R. M. D. Brydson, "Quantitative analysis of the microstructure of interfaces in steel reinforced concrete," *Cement and Concrete Research*, vol. 37, no. 12, pp. 1613–1623, 2007.